

# A connection between angular dependent phase ambiguities and the uniqueness of the partial wave decomposition

A. Švarc<sup>1,\*</sup>

Y. Wunderlich<sup>2</sup>, H. Osmanović<sup>3</sup>

M. Hadžimehmedović<sup>3</sup>, R. Omerović<sup>3</sup>, J. Stahov<sup>3</sup>,

V. Kashevarov<sup>4</sup>, K. Nikonov<sup>4</sup>, M. Ostrich<sup>4</sup>, L. Tiator<sup>4</sup>

R. Workman<sup>5</sup>

<sup>1</sup> *Rudjer Bošković Institute, Bijenička cesta 54, P.O. Box 180, 10002 Zagreb, Croatia*

<sup>2</sup> *Helmholtz-Institut für Strahlen- und Kernphysik der Universität Bonn, Nussallee 14-16, 53115 Bonn, Germany*

<sup>3</sup> *University of Tuzla, Faculty of Natural Sciences and Mathematics, Univerzitetska 4, 75000 Tuzla, Bosnia and Herzegovina*

<sup>4</sup> *Institut für Kernphysik, Universität Mainz, D-55099 Mainz, Germany and*

<sup>5</sup> *Data Analysis Center at the Institute for Nuclear Studies, Department of Physics, The George Washington University, Washington, D.C. 20052, USA*

(Dated: June 13, 2022)

Unconstrained partial-wave amplitudes obtained at discrete energies from fits to complete sets of experimental data may not vary smoothly with energy, and are in principle non-unique. We demonstrate how this behavior can be ascribed to the continuum ambiguity. Starting from the spinless scattering case, we demonstrate how an unknown overall phase depending on energy and angle mixes the structures seen in the associated partial-wave amplitudes making the partial wave decomposition non-unique, and illustrate it on a simple toy model. We then apply these principles to pseudo-scalar meson photoproduction and show that the non-uniqueness effect can be removed through a phase rotation, allowing a consistent comparison with model amplitudes. The effect of this phase ambiguity is also considered for Legendre expansions of experimental observables.

PACS numbers: PACS numbers: 13.60.Le, 14.20.Gk, 11.80.Et

Partial-wave analysis is a textbook method used to analyze experimental data (see for instance ref. [1]). In the quest for a unique set of amplitudes experimental programs have attempted to obtain complete sets of observables. In some cases, when fits from independent groups were compared, an energy-dependent phase was applied. On the other hand, it is well known that single-channel physical observables are invariant with respect to a more general energy- and angle-dependent phase rotation. This invariance is the so-called continuum ambiguity, and has been extensively analyzed in mid-70s through the mid-80s [2–4]. Most studies were made in the context of  $\pi N$  elastic scattering where the optical theorem and an application of elastic unitarity practically eliminate this as a source of non-uniqueness. Some other related studies [5, 6] concentrated on phase ambiguities in cases without a complete set of experimental data.

Programmatic studies of photoproduction experiments at Jefferson Lab, Mainz and Bonn are now producing the data required to do complete experiments, in terms of either helicity amplitudes or multipoles, motivating a reexamination of the ambiguities associated with multipole analyses. As mentioned, the main focus has been to handle angle-independent phase rotations at the level of partial waves [7–9]. We show that, contrary to well-behaved energy-dependent phase invariance, angle-dependent phase rotations mix partial waves, changing their analytic structure and producing a partial wave decomposition which is non-unique. The aspects of angle-dependent phase rotations we discuss here have

been mentioned, only in passing, at the conclusion of ref. [10]. In the following, we first demonstrate the interconnection of angle-dependent phase rotations and the non-uniqueness of partial wave decomposition. We then explore the effect of angle-dependent rotations in a case of practical interest, the single-energy analysis of a complete set of eta photoproduction pseudo-data comparing produced multipoles with known model results.

Recall that observables in single-channel reactions are given as a sum of products involving one (helicity or transversity) amplitude with the complex conjugate of another, so that the general form of any observable is  $\mathcal{O} = f(H_k \cdot H_l^*)$ , where  $f$  is a known, well-defined real function. The direct consequence is that any observable is invariant with respect to the following simultaneous phase transformation of all amplitudes:

$$H_k(W, \theta) \rightarrow \tilde{H}_k(W, \theta) = e^{i\phi(W, \theta)} \cdot H_k(W, \theta) \quad \text{for all } k = 1, \dots, n \quad (1)$$

where  $n$  is the number of spin degrees of freedom ( $n=1$  for the 1-dim toy model,  $n=2$  for  $\pi$ - $N$  scattering and  $n=4$  for pseudoscalar meson photoproduction), and  $\phi(W, \theta)$  is an arbitrary, real function which is the same for all contributing amplitudes.

As resonance properties are usually the goal of such studies, and these are identified with poles of the partial-wave (or multipole) amplitudes, we must analyze the influence of the continuum ambiguity not upon helicity or transversity amplitudes, but upon their partial wave decompositions. To simplify the study we introduce partial

waves in a simplified version than those found in Ref. [8]:

$$A(W, \theta) = \sum_{\ell=0}^{\infty} (2\ell+1) A_{\ell}(W) P_{\ell}(\cos \theta) \quad (2)$$

where  $A(W, \theta)$  is a generic notation for any amplitude  $H_k(W, \theta)$ ,  $k = 1, \dots, n$ . The complete set of observables remains unchanged when we make the following transformation:

$$\begin{aligned} A(W, \theta) \rightarrow \tilde{A}(W, \theta) &= e^{i \phi(W, \theta)} \\ &\times \sum_{\ell=0}^{\infty} (2\ell+1) A_{\ell}(W) P_{\ell}(\cos \theta) \\ \tilde{A}(W, \theta) &= \sum_{\ell=0}^{\infty} (2\ell+1) \tilde{A}_{\ell}(W) P_{\ell}(\cos \theta) \end{aligned} \quad (3)$$

We are interested in rotated partial wave amplitudes  $\tilde{A}_{\ell}(W)$ , defined by Eq.(3), and are free to introduce the

Legendre decomposition of an exponential function as:

$$e^{i \phi(W, \theta)} = \sum_{\ell=0}^{\infty} L_{\ell}(W) P_{\ell}(\cos \theta). \quad (4)$$

After some manipulation of the product  $P_{\ell}(x)P_k(x)$  (see refs. [11, 12] for details of the summation rearrangement) we obtain:

$$\tilde{A}_{\ell}(W) = \sum_{\ell'=0}^{\infty} L_{\ell'}(W) \cdot \sum_{m=|\ell'-\ell|}^{\ell'+\ell} \langle \ell', 0; \ell, 0 | m, 0 \rangle^2 A_m(W) \quad (5)$$

where  $\langle \ell', 0; \ell, 0 | m, 0 \rangle$  is a standard Clebsch-Gordan coefficient.

To get a better insight into the mechanism of multipole mixing, let us expand Eq. (5) in terms of phase-rotation Legendre coefficients  $L_{\ell'}(W)$ :

$$\begin{aligned} \tilde{A}_0(W) &= \mathbf{L}_0(\mathbf{W}) \mathbf{A}_0(\mathbf{W}) + L_1(W) \left[ \frac{1}{3} A_1(W) \right] + L_2(W) \left[ \frac{1}{5} A_2(W) \right] + \dots \\ \tilde{A}_1(W) &= \mathbf{L}_0(\mathbf{W}) \mathbf{A}_1(\mathbf{W}) + L_1(W) \left[ A_0(W) + \frac{2}{5} A_2(W) \right] + L_2(W) \left[ \frac{2}{5} A_1(W) + \frac{9}{35} A_3(W) \right] + \dots \\ \tilde{A}_2(W) &= \mathbf{L}_0(\mathbf{W}) \mathbf{A}_2(\mathbf{W}) + L_1(W) \left[ \frac{2}{3} A_1(W) + \frac{3}{7} A_3(W) \right] + L_2(W) \left[ A_0(W) + \frac{2}{7} A_2(W) + \frac{2}{7} A_4(W) \right] + \dots \\ &\vdots \end{aligned} \quad (6)$$

The consequence of Eqs. (5) and (6) is that angular-dependent phase rotations mix multipoles.

#### Toy model:

To better illustrate the process, we construct a simple toy model consisting of two partial waves, with one resonance per partial wave.

$$A(W, \theta) = T_S(W) + x T_P(W)$$

$$T_{S,P}(W) = \frac{a_{S,P}}{M_{S,P} - i \Gamma_{S,P}/2 - W} \quad (7)$$

$$x = \cos \theta \quad (8)$$

where

$$\begin{aligned} a_S &= 0.5 + i 0.4; \quad M_S = 1.535; \quad \Gamma_S = 0.15 \\ a_P &= 0.4 + i 0.3; \quad M_P = 1.44; \quad \Gamma_P = 0.1. \end{aligned}$$

We take a very simple linear rotation acting upon the full amplitude  $A(W, \theta)$ :

$$\mathcal{R}(x) = e^{i(2+0.5x)}, \quad (9)$$

and compare the partial-wave decompositions of the non-rotated and rotated amplitudes. In Fig. 1 we show the

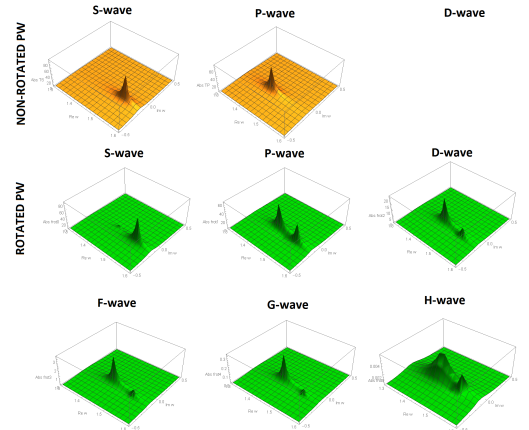


FIG. 1: (Color online) Toy model poles for linear rotation.

result.

On the basis of Eqs. (5) and (6) applied to the toy model, we observe several important features of the angle-dependent phase rotations:

1. The Legendre expansion of the angle-dependent phase rotation, given by Eq. (4), has, in princi-

ple, an infinite number of terms. However, it can be shown (see ref. [12]) that in cases of simpler rotations, higher order terms rapidly become very small.

2. The lowest rotation coefficient  $L_0(W)$  transforms only  $A_\ell(W)$  to  $\tilde{A}_\ell(W)$ . Hence, for angle-independent rotations, only the 0-th order Legendre coefficient survives, and this does not mix multipoles.
3. Even the simplest quickly converging rotations, with only a few Legendre coefficients significantly greater than zero, will mix multipoles. The degree of mixing rises with the complexity of the angular rotation.
4. Through the influence of the angle-dependent phase rotation, no new pole positions are created, but resonances with the same pole positions appear in new and therefore multiple partial waves

### Conclusions:

Without fixing the free continuum ambiguity phase  $\phi(W, \theta)$ , the partial wave decomposition  $A_\ell(W)$  defined in Eq. (2) is non-unique. To compare different partial-wave analyses, it is essential to match the continuum ambiguity phase; otherwise the mixing of multipoles is yet another, uncontrolled, source of systematic errors.

One other interesting effect can be observed. The toy-model  $A(W, \theta)$  truncated at  $L = 1$  leads to 'data' for the differential cross section whose Legendre-expansion

$$\sigma_0(W, \theta) = |A(W, \theta)|^2 = \sum_{n=0}^2 a_n(W) P_n(\cos \theta), \quad (10)$$

would be precisely truncated at  $2L = 2 * 1 = 2$ , i.e. all Legendre coefficients up to and including  $a_2$  would be non-vanishing, with all higher coefficients, i.e.  $a_3$  and above, being precisely zero. If one then defined a new amplitude, with the angle-dependent phase (9) multiplied into the original truncated amplitude, we would end up with an, in principle, infinite partial-wave expansion for the rotated amplitude (which, however, converges quite well for the higher  $\ell$ ). In fact, the rotation (9) itself turns out to be truncated at  $L' = 5$  to a very good approximation, since all of its Legendre coefficients  $L' \geq 6$  have moduli within the range of  $10^{-7}$  or less.

Now, one might naively expect the Legendre-expansion of the data (10) to show non-vanishing Legendre-coefficients up to and including  $2(L + L') = 2 * (1 + 5) = 12$ , once the rotated amplitude has been inserted. This, however, this is not what happens. Since the phase (9) has modulus 1 for all  $x$ , it will leave the cross section invariant. The data simply do not change. Since the original data are truncated at  $2 * 1 = 2$ , by construction, the rotated data will be as well. However, the rotated amplitude itself is manifestly not truncated. Furthermore,

higher Legendre-coefficients  $a_{\ell \geq 3}$  are bilinear hermitean forms, depending on the rotated partial waves. All this implies that a cancellation-effect has to set all 'rotated' Legendre coefficients  $a_3, \dots, a_{12}$  to zero. The rotation (9) has generated higher partial waves in such a 'finely tuned' way that this is indeed possible.

Having explored a simple toy model, we next consider a more realistic analysis of precise pseudo-data generated from an existing fit to data for this reaction. We perform unconstrained,  $L_{max} = 8$  truncated single-energy analyses on a complete set of observables for  $\eta$  photoproduction given in the form of numeric data created using the MAID15a model [13]:  $d\sigma/d\Omega$ ,  $\Sigma d\sigma/d\Omega$ ,  $T d\sigma/d\Omega$ ,  $F d\sigma/d\Omega$ ,  $G d\sigma/d\Omega$ ,  $P d\sigma/d\Omega$ ,  $C_x d\sigma/d\Omega$ , and  $O_x d\sigma/d\Omega$ . All higher multipoles are put to zero. The fitting procedure finds solutions which are non-unique, and we obtain many solutions depending on the choice of initial parameters in the fit.

In Fig. 2, which is only a snapshot of an infinite number of possible solutions, we show examples of three very different sets of multipoles which fit the complete data set equally well to a high precision: two discrete and discontinuous ones obtained by setting the initial fitting values to the MAID16a [14] ( $SE^{16a}$ ) and Bonn-Gatchina [15] ( $SE^{BG}$ ) model values (blue and red symbols respectively). The generating MAID15a model [13] is displayed as full and dashed black continuous lines.

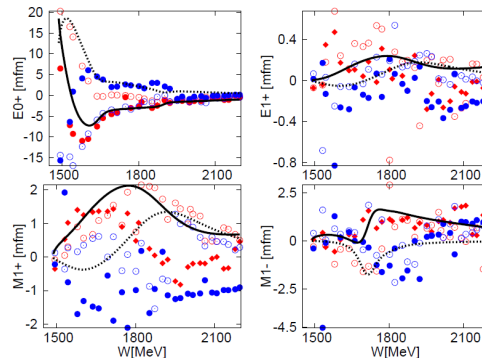


FIG. 2: (Color online) Plots of the  $E_{0+}$ ,  $M_{1-}$ ,  $E_{1+}$ , and  $M_{1+}$  multipoles. Full and dashed black lines give the real and imaginary part of the MAID15a generating model.

Discrete blue and red symbols are obtained with the unconstrained,  $L_{max} = 8$  fits of a complete set of observables generated as numeric data from the MAID15a model of ref. [13], with the initial fitting values taken from the MAID16a [14] and the Bonn-Gatchina [15] models respectively. Filled symbols represent the real parts and open symbols give the imaginary parts.

We know from Eq.(1) that equivalent fits to a complete set of data must be produced by helicity amplitudes with different phases. Therefore, in Fig. 3, we construct the helicity amplitudes corresponding to all three sets of multipoles from Fig. 2 at one randomly chosen energy  $W = 1660.4$  MeV.

We see that all three sets of helicity amplitudes indeed

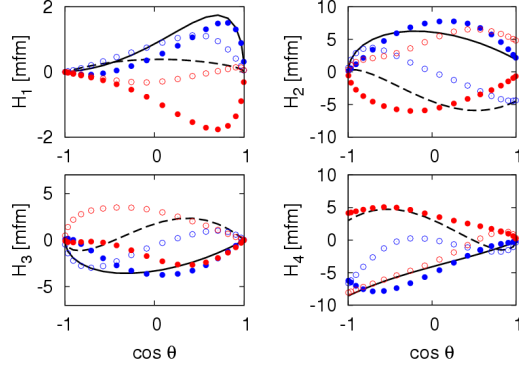


FIG. 3: (Color online) We show three sets of helicity amplitudes for all three sets of multipoles at one randomly chosen energy  $W = 1660.4$  MeV.

are different, but the discontinuity of multipole amplitudes, observed in Fig. 2, is not reflected in a plot of helicity amplitudes at a single energy.

If instead we plot an excitation curve of all four helicity amplitudes at the randomly chosen angle corresponding to  $\cos \theta = 0.2588$ , we obtain the result shown in Fig. 4.

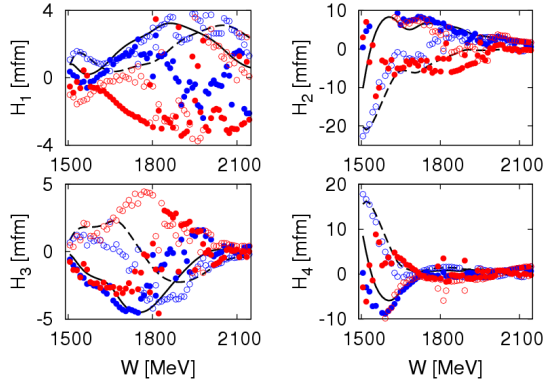


FIG. 4: (Color online) Excitation curves of all helicity amplitudes, for all three sets of multipoles, at one randomly chosen value of  $\cos \theta = 0.2588$  MeV.

We see that the the excitation curve of helicity amplitudes in this case remains continuous only for the generating model MAID15a. For both single-energy solutions it shows a discontinuity between neighbouring energy points.

To reveal the source of this discontinuity, we compare helicity amplitudes at one randomly chosen value of  $\cos \theta = 0.2588$ , at a randomly chosen energy of  $W = 1660.4$  MeV. In Fig. 5, the four helicity amplitudes are plotted in the complex plane for the generating solution and the result of a particular single-energy fit.

We see that all four helicity amplitudes have identical moduli and relative phases, but the two sets differ by an overall rotation. This comparison holds for each angular

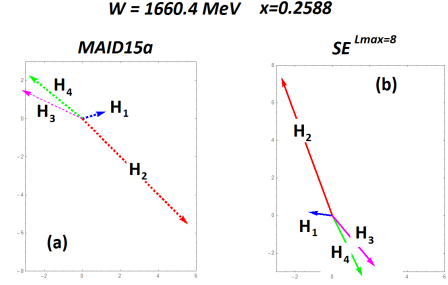


FIG. 5: (Color online) We show all helicity amplitudes for generating solution in Fig. (a) and for one out of two discussed  $L_{max} = 8$  unconstrained solutions in Fig.(b) at one randomly chosen energy of  $W = 1660.4$  MeV, and one randomly chosen value of  $\cos \theta = 0.2588$ .

point at any arbitrarily chosen energy.

This leads to the following understanding of the very different multipole solutions:

*When we perform an unconstrained SE PWA, each minimization is performed independently at individual energies, and the phase is undetermined. So, at each energy the fit chooses a different angle dependent phase, and creates different, discontinuous numerical values for each helicity amplitude, producing discontinuous sets of multipoles.*

However, the invariance with respect to phase rotations offers a possible solution. We introduce the following angle-dependent phase rotation:

$$\tilde{H}_k^{SE}(W, \theta) = H_k^{SE}(W, \theta) \cdot e^{i\Phi_{H_2}^{15a}(W, \theta) - i\Phi_{H_2}^{SE}(W, \theta)} \quad (11)$$

$$k = 1, \dots, 4$$

where  $\Phi_{H_2}^{SE}(W, \theta)$  is the phase of any single-energy solution and  $\Phi_{H_2}^{15a}(W, \theta)$  is the phase of generating solution MAID15a. Applying this rotation replaces the discontinuous  $\Phi_{H_2}^{SE}(W, \theta)$  phase from any SE solution with the continuous  $\Phi_{H_2}^{15a}(W, \theta)$  MAID15a phase. All four helicity amplitudes would be rotated by this single phase.

The resulting rotated single-energy helicity amplitudes are compared with generating MAID15a amplitudes in Fig. 6.

We see that rotated helicity amplitudes of both single-energy solutions are now identical to the generating MAID15a helicity amplitudes. Thus, the previously different sets of discrete, discontinuous single-energy multipoles are, after phase rotation, now equal to multipoles of the generating solution. So, we have constructed a way to generate up-to-a-phase unique solutions in an unconstrained PWA of a complete set of observables.

Let us summarize by affirming that taking into consideration the angle dependent continuum ambiguity phase is not only an academic issue; it is essential. It introduces up-to-a phase uniqueness. First of all, it influences partial wave decompositions, on the other hand it enables one to obtain an up-to-a phase unique solution in the unconstrained PWA of a complete set of observables.

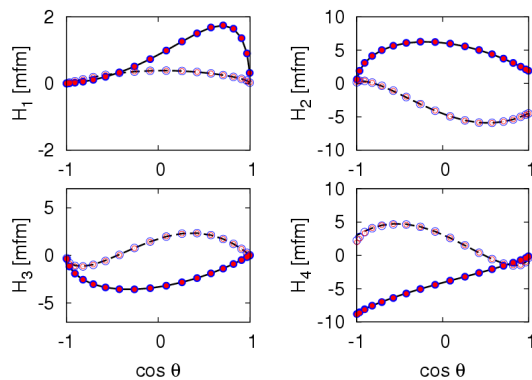


FIG. 6: (Color online) We show all three sets of rotated helicity amplitudes and generating helicity amplitudes at one randomly chosen energy  $W = 1660.4$  MeV. The figure coding is the same as in Fig. 2.

Let us stress that the continuum ambiguity phase is not just a mathematical fiction. It definitely exists, and it can in principle be exactly determined in coupled-channel calculations. When only one channel is analyzed, unitar-

ity constraints relating real and imaginary parts of the partial wave T-matrices are lost after the first inelastic threshold opens, but it is automatically restored when all channels are included in coupled-channel calculations (uncontrolled loss of flux in one channel is controlled by including all of them).

In conclusion, the continuum ambiguity must, in some way, be taken into account to actually obtain a partial-wave solution. Without fixing the overall angle and energy dependent phase, a whole class of solutions exists, connected via rotations. As we have seen in Eqs. (5) and (6) and in a simple toy model, these rotations do not create new pole positions but may put poles into partial waves having different quantum numbers. Obtaining the correct quantum numbers requires a method to remove this ambiguity. This requires theoretical input beyond a complete set of experimental data, such as unitarity or the modeling of unfitted higher partial waves.

This work was supported by the Deutsche Forschungsgemeinschaft (SFB 1044). The work of RW was supported by the U.S. Department of Energy grant DE-SC0016582.

- 
- [1] A.D. Martin and T.D. Spearman: Elementary Particle Theory, North-Holland Publishing Company, Amsterdam 1970.
  - [2] D. Atkinson, P.W. Johnson and R.L. Warnock, Commun. mat. Phys. **33** (1973) 221.
  - [3] J.E. Bowcock and H. Burkhard, Rep. Prog. Phys. **38** (1975) 1099.
  - [4] D. Atkinson and I.S. Stefanescu, Commun. Math. Phys. **101**, 291 (1985).
  - [5] N.W. Dean and P. Lee, Phys. Rev. D **5**, 2741 (1972).
  - [6] G. Keaton and R. Workman, Phys. Rev. C **54**, 1437 (1996).
  - [7] A.V. Anisovich, R. Beck, E. Klempt, V.A. Nikonov, A.V. Sarantsev, U. Thoma, Eur. Phys. J. **A48**, 15 (2012).
  - [8] L. Tiator, D. Drechsel, S. S. Kamalov and M. Vanderhaeghen, Eur. Phys. J. ST **198**, 141 (2011).
  - [9] A. M. Sandorfi, S. Hoblit, H. Kamano, and T.-S. H. Lee, J. Phys. G: Nucl. Part. Phys. **38** (2011) 053001.
  - [10] A.S. Omalaenko, Sov. Jour. Nucl. Phys. **34**(3) (1981) 406-411.
  - [11] J. Dougall, Glasgow Mathematical Journal, **1** (1952) 121-125.
  - [12] Y. Wunderlich: The complete experiment problem of pseudoscalar meson photoproduction in a truncated partial wave analysis", Dissertation zur Erlangung des Doktorgrades (Dr. rer. nat.) der Mathematisch-Naturwissenschaftlichen Fakultät der Rheinischen Friedrich-Wilhelms-Universität, Bonn 2017.
  - [13] V. L. Kashevarov, L. Tiator, M. Ostrick, Bled Workshops Phys., **16**, 9 (2015).
  - [14] V. L. Kashevarov, L. Tiator, M. Ostrick, JPS Conf. Proc. **13**, 020029 (2017).
  - [15] <http://pwa.hiskp.uni-bonn.de/>
  - [16] R.L. Workman, L. Tiator, Y. Wunderlich, M. Doering, H. Haberzettl, Phys. Rev. C **95**, 015206 (2017).
  - [17] J. Nys, V. Mathieu, C. Fernandez-Ramirez, A. N. Hiller Blin, A. Jackura, M. Mikhasenko, A. Pilloni, A. P. Szczepaniak, G. Fox, J. Ryckebusch, Phys. Rev. D **95**, 034014 (2017).
  - [18] R.L. Workman, M.W. Paris, W.J. Briscoe, L. Tiator, S. Schumann, M. Ostrick, and S.S. Kamalov, Eur. Phys. J. A **47**, 143 (2011).
  - [\*] Corresponding author: alfred.svarc@irb.hr